PNL-SA-7809
CONF-790749--2

MASTER

IMPROVEMENT OF SPUTTERED OXIDE COATING ADHERENCE AND INTEGRITY FOR TURBINE AIRFOIL APPLICATIONS*

M.A. Bayne, R. Busch
Pacific Northwest Laboratory**
Richland, Washington 99352

J.W. Fairbanks
US Department of Energy
Division of Fossil Fuel Utilization
Washington, DC 20545

and

J.W. Patten
Pacific Northwest Laboratory**
Richland, Washington 99352

Two aspects of the durability of modified ZrO_2 ceramic thermal barrier coatings for gas turbine airfoils are being investigated in this program. First, adherence of coatings of these materials has historically been difficult to achieve due to mismatch in thermal expansion coefficients and other properties between ceramic coatings and metallic substrates. Second, if the ceramic coatings are discontinuous, as for many plasma sprayed coatings, then condensate from the combustion environment may permeate the coating and volume changes in this condensate during subsequent service cycles may produce coating spallation. The adherence problem is approached in this work by seeking to sputter deposit ceramic coatings over either sputter-etched, closely spaced, high aspect ratio substrate surface cones or by sputter depositing ceramic coatings over sputtered CoCrAlY coatings containing a very high density of columnar voids (leaders). The objective in both instances is to provide a compliant fibrous metal attachment between metal substrate and ceramic coating to absorb property mismatches. Progress in providing the fibrous layers and preliminary evaluation of adherence are discussed. The permeability problem is approached both by providing a continuous and impervious ceramic overlayer, and by coating the ceramic layer with a continuous and impervious metal sealing layer that is not required to provide structural strength or insulation. The merits of both of these approaches and preliminary experimental results are discussed.

*This research is supported by US Department of Energy, under Contract EY-76-C-06-1830.
**Operated by Battelle Memorial Institute.

DISCLAIMER

INTRODUCTION

The durability of directly fired heat engines operating on minimally processed coal-derived liquid fuels is dependent on the hot-corrosion/erosion resistance of combustion zone components. The inherent superior resistance of some ceramic materials to very aggressive hot-corrosion and erosion environments suggests their consideration for gas turbine and diesel engine combustion zone component applications.[1-3] Although the use of monolithic ceramics in industrial/utility gas turbine engine hot sections does not appear to be a near-term or mid-term solution[2] it is felt that many of the advantages of ceramics for engine durability can be achieved by applying the ceramics as coatings on metal substrates and relying on the metal substrates to accommodate the mechanical loading.

The principal problems to be solved may be classified as relating either to corrosion/erosion/thermal protection or to coating adherence. The protective nature of several ceramic coatings has been established,[1-12] but adherence remains a critical technical problem that must be solved before ceramic coatings become useful in very aggressive environments.[13,14] Therefore, the research discussed here is directed primarily at the adherence problem, with related implications for corrosion protection.

The adherence problem may further be divided into questions regarding a) deposit-substrate bond strength, b) bond area between coating and substrate, c) the inability of brittle ceramic materials (particularly continuous coatings) to accommodate modulus and thermal expansion mismatches with metal substrates, or d) entrainment of corrosion products or condensates in coating porosity followed by thermal expansion induced stressing and spalling of the surrounding ceramic coating on thermal cycling.[3]

Routine sputter deposition techniques include ion bombardment etching of the substrate immediately prior to sputter deposition which normally produces extremely good deposit-substrate bond strengths,[15] Figure 1. However, even if bond strength is high, the force required to separate a coating from its substrate is limited by the product of the total cross-sectional area of the bond and the strength of the substrate or the deposit, whichever is weaker. Therefore, if a coating is bonded to a fibrous surface, the fiber area must be maximized, i.e. fibers must be as numerous and as closely packed as possible. The research described in this paper, therefore, is concerned, first, with accommodation of expansion and modulus mismatches at the coating-substrate interface and, second, with preventing coating penetration and impregnation by corrosion products or condensates. Solutions to these problems are being sought with coating designs having a high fraction of the substrate surface area bonded to the coating.

APPROACH

At Pacific Northwest Laboratory (PNL) accommodation of interfacial mismatches is being attempted with two coating designs. The first design, illustrated in Figure 2, involves producing densely packed, high aspect ratio cones on the substrate surfaces by ion etching and selective "seeding," or introduction of low yield or high melting point elements to the substrate

surface.[16-22] Subsequent sputter deposition of a ceramic coating on such a fibrous substrate would produce a columnar ceramic structure, with individual growth columns being separated from each other like densely packed fibers.

The second design, illustrated in Figure 3, involves sputter depositing a metal layer such as a CoCrAlY alloy directly on the metal substrate to produce a fibrous bond coat with a very high density of columnar voids or leaders. A ceramic layer sputtered over this type of layer is expected to be similar to the ceramic layer discussed for the first coating design.

Prevention of coating penetration or impregnation would be required with both coating designs, and a continuous "closeout" layer is planned for this purpose. This layer may either be metallic or ceramic. Here a continuous ceramic layer may be practical because of elimination of interfacial mismatches. However, requirements for resistance to foreign particle damage may dictate that a metallic layer be used.

SUBSTRATE SURFACE STRUCTURE MODIFICATION BY ION ETCHING

Apparatus and Procedure

An existing PNL triode sputtering apparatus was modified to accept an 8-specimen array, Figure 4, for substrate surface structure modification experiments. This apparatus permits two of the primary variables for cone formation, i.e. substrate temperature and voltage, to be examined at several levels, e.g. four temperatures and two voltages in each experiment. The remaining variables (current density, etching time, sputtering atmosphere, deliberate surface contaminants, and substrate material) are examined in subsequent experiments. Each of the two arrays supports four specimens and is equipped with a heater at the free end and air cooling at the fixed end. Each specimen location is provided with a thermocouple that is inserted into a small hole in the 1.91 cm diameter specimen, which is attached to the arm with a bolt. Only the faces of the specimens are emersed in the plasma, with the support arms and associated hardware being protected by a flat plate plasma shield.

Typical experimental procedures were as follows:

1. Prepare specimens by lapping on #600 grit sand paper.
2. After evacuation to $< 3 \times 10^{-4}$ Pa (2×10^{-6} torr), check the outgassing rate by valving off the pumping station.
3. If $\Delta P/\Delta t < -3 \times 10^{-3}$ Pa/min for five minutes, backfill the system with $\simeq 0.40$ Pa (3×10^{-3} torr) krypton gas.
4. Apply power to heaters.
5. Set plasma voltage at 40 V and ignite plasma with thermionic emitter.

6. Raise plasma current to the predetermined operating level (40-80 amps) by increasing electron emission from the hot tungsten filament.

7. Add oxygen if required.

8. Apply voltage to seed material electrode if required.

9. Apply bias voltage to etch the substrate for the specified time.

10. At the end of the etch, shut off the system and allow the specimens to cool to room temperature prior to opening the vacuum system.

Analysis consisted of an initial visual examination, weight and thickness loss measurements, and scanning electron microscopy to determine the size and density distribution of any growth features.

Results and Discussion

In general, sample temperature had the greatest influence on the etched surface structure. The effects of specimen temperature on surface structure reverse of IN718 are shown in Figures 5, 6 and 7 for three etch voltages without foreign element seeding. A typical surface prior to ion etching is shown in Figure 5c,d. The density and height of the conical growth features increase with temperature increases into the 300-350°C range and remain relatively constant with further temperature increases. Temperatures above 350°C produced small-scale roughening of two types--stepped planar layers and ridges oriented perpendicular to the substrate surfaces. However, with temperatures up to 600°C, no conical features with the desired density and aspect ratio were observed. This was taken as an indication that up to about 600°C the approximate 6% refractory metal content in the IN718 alloy is not effective in producing nucleation sites for cone growth. Higher temperatures have not yet been investigated because of limitations in the equipment. However, higher temperatures may produce sufficient increases in surface mobility of these refractory metals to stimulate cone growth.

Foreign atom seeding from an external source was utilized in an attempt to introduce nucleation sites for cone growth. Foreign atoms included tantalum, molybdenum, oxygen, carbon, and various combinations of these.

Tantalum was added with a flux between 6×10^{14} and 2×10^{15} atoms/cm^2/sec with oblique incidence in the temperature range of 400 to 585°C. The IN718 removal rate was about 6×10^{16} atoms/cm^2/sec so that up to 2% seeding was achieved. Surface structures were similar to those obtained at comparable temperatures without seeding, Figure 8.

When molybdenum was added with oxygen, either obliquely or with fairly normal incidence, a small number of cones (less than 40/cm^2) with aspect ratios less than one were obtained, Figure 9. Molybdenum flux was 2×10^{15} atoms/cm^2/sec and IN718 removal rate was 3×10^{16} atoms/cm^2/sec. The highest temperature attained was 525°C.

Oxygen additions to the sputtering gas for seed material influenced the surface topography and produced cones of the desired number density in some cases, Figure 10c. Perhaps because of the reactive nature of the seed material, etch bias voltage had a larger affect on cone formation than previously observed. At 500 volts, cone density was < 20 cm^2, at 1000 eV density was about 100/cm^2, and at 1500 eV bias, density was greater than 50,000/cm^2 with a high density of small cones superimposed on a small number of very large cones. This observation may be related to the decrease in sputtering yield of IN718 with increasing O_2 partial pressure at temperatures near 400°C, Figure 11. Temperatures greater than 500°C produced varied surface topographies, some of which included cones of the desired aspect ratio and density, Figure 12c. Reproducibility however, was extremely poor indicating that a factor other than oxygen seeding may have been responsible for the cone structures.

Residual gas analysis revealed an unusually high CO concentration for some of the experiments with O_2 seeding, indicating the possibility of carbon contamination on the substrate surface prior to or during etching. Therefore, an experiment was performed in which Starrett® oil thinned with toluene was placed on the surface of the substrates just prior to etch experiments. The 500 eV bias results were similar to previous nonexternally seeded etch results, Figure 13. Large cones formed with 1000 eV bias had an appearance suggesting that they were formed early in the etch and then sputtered away, Figure 14. The temperature dependence of the cone density was < 200/cm^2 at 360°C, > 300/cm^2 at 430°C, and > 600/cm^2 at 460°C. At 515°C the substrate surface was nearly covered with cones, with their density estimated at > 3000/cm^2. Because the seeding was not continuous, and sputter etching of the cones had occurred, it is only possible to estimate their original height, but some appear to have approached 25 μm in height.

Future Work

Because of the unexpected difficulty encountered in obtaining reproducible metallic cone surface structures, investigation of ceramic overlayers has not yet been initiated. Experiments with substrate surface temperatures, up to 800°C, will be conducted next in an attempt to produce the desired surface structure. Also, means of continuously depositing dense fluxes of carbon, molybdenum and tantalum as seed materials will be sought. If suitable surface structures are obtained, then deposition of ceramic overlayers and closeout layers will follow.

®The L.S. Starrett Company, Athol, Massachusetts.

DEVELOPMENT OF METALLIC BOND COATS WITH LARGE NUMBERS OF COLUMNAR VOIDS OR LEADERS

Sputtering Apparatus and Procedures

Early PNL research directed towards producing high integrity sputter-deposited CoCrAlY coatings on marine gas turbine first stage airfoils indicated that most line-of-sight deposition techniques resulted in columnar growth structures in the coatings, with voids between adjacent growth columns that often extend entirely through the coating thickness. These voids are commonly referred to as leaders, and have recently been associated with a geometrical shadowing mechanism.[23] Sputtering parameters conducive to the formation of coatings with a very large number of leaders oriented perpendicular to the substrate surface were used to produce the initial fibrous bond coats in sputtering equipment similar to that discussed in detail previously.[24-27] A modified sputtering chamber capable of coating seven substrates simultaneously was used to deposit about 50 μm of CoCrAlY as a fibrous bond coat onto heavy-walled stainless steel tubing, Figure 15.

A high-rate planar magnetron sputtering apparatus[28] was designed and built specifically to allow deposition of the stoichiometric oxides required for this research at deposition rates of approximately 0.0025 cm/hr. A schematic of this apparatus is shown in Figure 16. Typical sputtering performance is indicated in Figure 17.

Results and Discussion

As-deposited CoCrAlY surface topography is shown in the SEM photographs, Figure 18. Some of the specimens were ion etched to determine if the columnar structure could be enhanced to produce high aspect ratio cones. The SEM photograph in Figure 19 indicates that growth columns were rounded by ion etching rather than being accentuated or developing high aspect ratio cones. Several etched and unetched specimens were then sputter coated with ~ 18 μm of stabilized zirconia. SEM photographs of this coating over an unetched CoCrAlY bond coat indicate that the desired fibrous ceramic layer was achieved, Figure 20.

Several of these fibrous bond coated tube specimens were subjected to thermal shock screening tests involving radiant heating to 950°C in 70 seconds followed by either water quenching or forced air cooling to 150°C. The most severe test included four thermal cycles, two with air cooling and two with water quench. No evidence of coating fracture or spalling was observed after this test, Figure 20.

Future Work

If these coatings can be reproduced, the next efforts will be directed at producing adherent outer sealing of "closeout" layers, thermal shock testing of the complete coating system, and delivery of coated specimens for preliminary burner rig testing.

CONCLUSIONS

A variety of cone structures have been produced by ion etching substrate surfaces. However, none of these structures have been both reproducible and displayed sufficiently closely packed high aspect ratio cones to be promising as accommodation layers. Ion etching surface temperatures and surface seeding have not yet been completely explored, however.

CoCrAlY bond coats with large numbers of columnar voids or leaders, however, were readily obtained and preliminary evaluation of structures indicate that the desired accommodation geometry has been achieved. Further, ceramic coatings were applied over these fibrous or segmented bond coats and were adherent during moderately severe cyclic thermal shock testing. Ceramic or metallic sealing on closeout layers still must be applied to the outer surface of these systems before they are ready for hot corrosion testing.

We gratefully acknowledge the valuable contributions of Sputtering Technologist, J.W. Johnston; and Scanning Electron Microscoptist, H.E. Kjarmo. In addition, the preparation of this manuscript would not be possible without the expertise of A.M. Dyken and D.J. Benson.

REFERENCES

1. Dapkunas, S.J. and Clarke, R.L. Evaluation of the Hot-Corrosion Behavior of Thermal Barrier Coatings. Naval Ship Research and Development. November 1974. NSRDC-4428.

2. Clarke, R.C., and Dapkunas, S.J. Behavior of Stabilized Zirconia in Molten Sodium Sulphate, Naval Ship Research and Development Center. November 1974. NSRDC-4406.

3. Palko, J.E., Luthra, K.L, and McKee, D.W. Evaluation of Performance of Thermal Barrier Coatings Under Simulated Industrial/Utility Gas Turbine Conditions, Final Report, May 1978, DOE Contract EC-77-C-05-5402.

4. Busch, R. Develop Sputter Deposited, Graded Metal-ZrO_2 Coating Technology for Application to Turbine Hot Section Components. Prepared for The Naval Sea Systems Command by Battelle, Pacific Northwest Laboratories, Richland, Washington. October 11, 1976. NAVSEA SYSCOM Contract N00024-75-C-4333.

5. Kvernes, I. and Fartum, P. Thin Solid Films, 53 (1978) 259-269.

6. Liebert, C.H., and Stepka, F.S. Potential Use of Ceramic Coating as a Thermal Insultation on Cooled Turbine Hardware. 1976. NASA TM X-3352.

7. Liebert, C.H., et al. Durability of Zirconia Thermal-Barrier Ceramic Coatings on Air-Cooled Turbine Blades in Cyclic Jet Engine Operation. 1976. NASA TM X-3410.

8. Stecura, S. Two-Layer Thermal Barrier Coating for Turbine Airfoils - Furnace and Burner Rig Test Results. 1976. NASA TM X-3425.

9. Butze, H.F., and Liebert, C.H. Effect of Ceramic Coating of JT8D Combustor Liner on Maximum Liner Temperatures and Other Combustor Performance Parameters. January 1977. NASA TM X-73581.

10. Stoner, B. Study of Thermal Barrier Coatings for High Temperature Gas Turbine Engines. Contract NAS3-20067, United Technologies, Power Systems Division. February 1977. NASA CR-135147.

11. Levine, S.R., and Clark, J.S. Thermal Barrier Coatings - A Near-Term High Payoff Technology. ERDA Workshop on Ceramics for Advanced Heat Engines, Orlando, Florida. January 24-26, 1977. CONF-770110.

12. Muszar, K.E. Development and Evaluation of A Graded Metal-Ceramic Thermal Barrier for Gas Turbine Components. Detroit Diesel Allison Division, General Motors Corporation, Indianapolis, Indiana. July 31, 1975. Final Report for Naval Air Systems Command, Department of the Navy Contract N62269-73-C-0357.

13. Becher, P.F., et al. Thin Solid Films, 53 (1978) 225-232.

14. Liebert, C.H. and Stepka, F.S., Industry Tests of NASA Aramic Thermal Barrier Coatings, NASA Technical Paper 1425, Lewis Research Center, Cleveland, Ohio, June 1979.

15. McClanahan, E.D., et al. "State-of-the-Art for High-Rate Sputter Deposition," presented at the Government-Industry Workshop on Alternatives for Cadmium Electroplating in Metal Finishing, National Bureau of Standards, Gaithersburg, MD, October 4-6, 1977.

16. Wehner, G.K., Hajicek, D.J. "Cone Formation on Metal Targets During Sputtering." J. Appl. Phys. 42, 1145-1149, 1971.

17. Wehner, G.K., Yurista, Bhstia, S., and Housland, C. "Whiskers, Cones and Pyramids Created in Sputtering by Ion Bombardment." To be published in J. Appl. Phys.

18. Navinsek, B. "Sputtering-Surface Changes Induced by Ion Bombardment." Prog. in Surface Science 7(49), 1976.

19. Chaudhari, P. "Hillock Growth in Thin Films." J. Appl. Phys., 45(10): 4339-4346, October 1974.

20. Evans, C.C. Whiskers, Monograph ME/8, Mills & Boon Ltd., London, 1972.

21. Bunshah, R.F. and Juntz, R.S. "Influence of Condensation Temperature on Microstructure and Tensile Properties of Titanium Sheet Produced by High-Rate Physical Vapor Deposition Process." Met. Trans. 4:21-26, January 1973.

22. Okuyama, F. "Vapor-Grown Tungsten Whiskers Induced by Vacuum Discharges." J. Appl. Phys. 45(10):4239-4241, October 1974.

23. Patten, J.W. "The Influence of Surface Topography and Angle of Adatom Incidence on Growth Structure in Sputtered Cr." presented at the International Conference on Metallurgical Coatings," April 23-27, 1979, to be published in Thin Solid Films.

24. Patten, J.W., Hays. D.D., Moss, R.W., and Fairbanks, J.W., Proceedings of the 1977 Tokyo Joint Gas Turbine Congress, Gas Turbine Society of Japan, October 1977, 527-537.

25. Patten, J.W. and Hays, D.D. "Application of High-Rate Sputtering Technology to the Formation of Hot Corrosion-Resistant Metallic Coatings on Marine Gas Turbine First-Stage Vanes and Blades," presented at conference Gas Turbine Materials in a Marine Environment, US Naval Ship Engineering Center and UK Ship Dept. at Bath University, Bath, England, September 20-23, 1976.

incorporate into text + remove from list

this may be incorporated as in-text ref + removed from ref list

26. Fairbanks, J.W., Patten, J.W., Busch, R., and McClanahan, E.D. "High-Rate Sputter Deposition of Protective Coatings on Marine Gas Turbine Hot-Section Superalloys," Proceedings of the 1974 Gas Turbine Materials in the Marine Environment Conference, Battelle Metals and Ceramics Information Center MCIC 75-27, Castine, Maine, July 1974.

27. Patten, J.W., et al. "Preliminary Report on the Sputter Deposition of Platinum Coatings on Superalloy Pins," NAVSEA Contract N00600-73-C-0583, Battelle-Northwest, Richland, WA, January 25, 1974.

28. Kirou, K.I., Georgiev, S.S., Ivanov, N.A., and Minchev, G.M. "The Characteristics of a Modified Planar-Magnetron Sputtering Source." Vacuum 128(4):183-186, 1978.

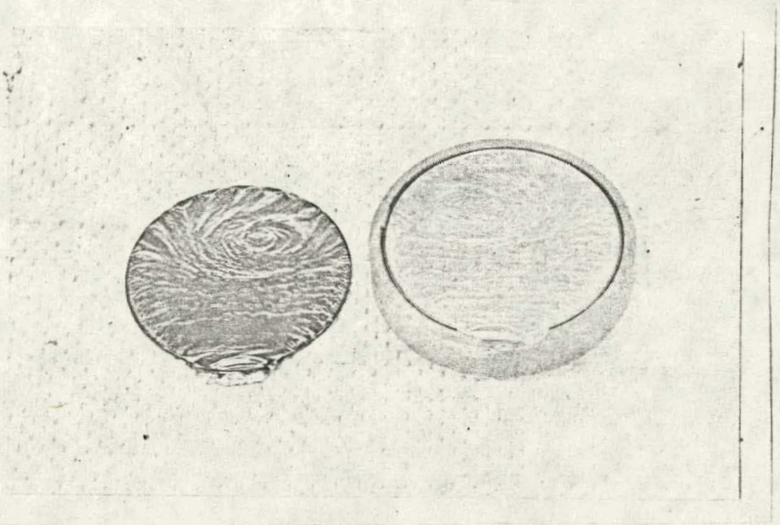

FIGURE 1

Demonstration of deposit-substrate bond strength. A titanium bond coat (<0.001" thick) was sputter deposited onto a ceramic substrate, followed with about 0.015" of copper. The stress induced separation did not occur at either the copper-titanium interface or titanium-ceramic interface. Rather, the fracture occurred about ≃0.08" inside the ceramic substrate. Shown is the fractured ceramic substrate (right) and the back side of the deposit (left) with the layer of ceramic material attached.

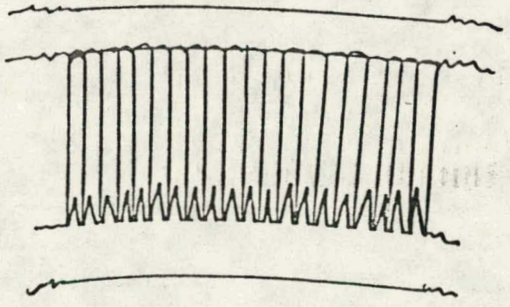

FIGURE 2

Model of a conical substrate (or bond coat) surface/ceramic coating system to improve adherence. In this concept, conical growth features are formed on the surface of the bond coat or substrate to provide mechanical keying and to promote columnar growth of the ceramic deposit for improved adherence. To enhance the corrosion/errosion properties of the coating system, an impervious closeout layer is required. This may be either metallic or ceramic.

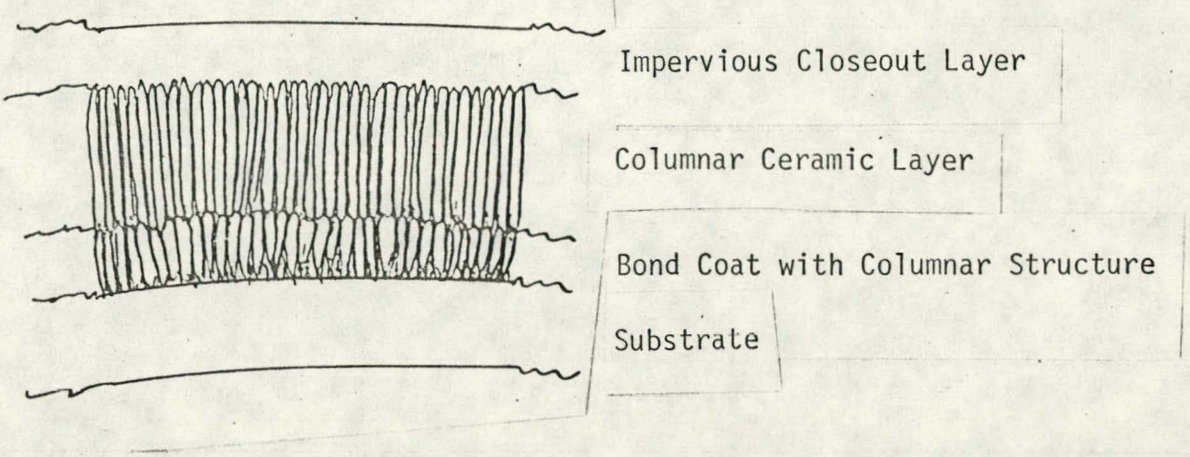

FIGURE 3

Model of bond coat with columnar defects/ceramic coating system to improve adherence. In this concept, a metallic bond coat is deposited with a high incidence of leader type defects to promote columnar growth of the ceramic deposit and to provide a compliant inner layer to improve adherence. To enhance the corrosion/errosion properties of the coating system, an impervious closeout layer is required. This may be either metallic or ceramic.

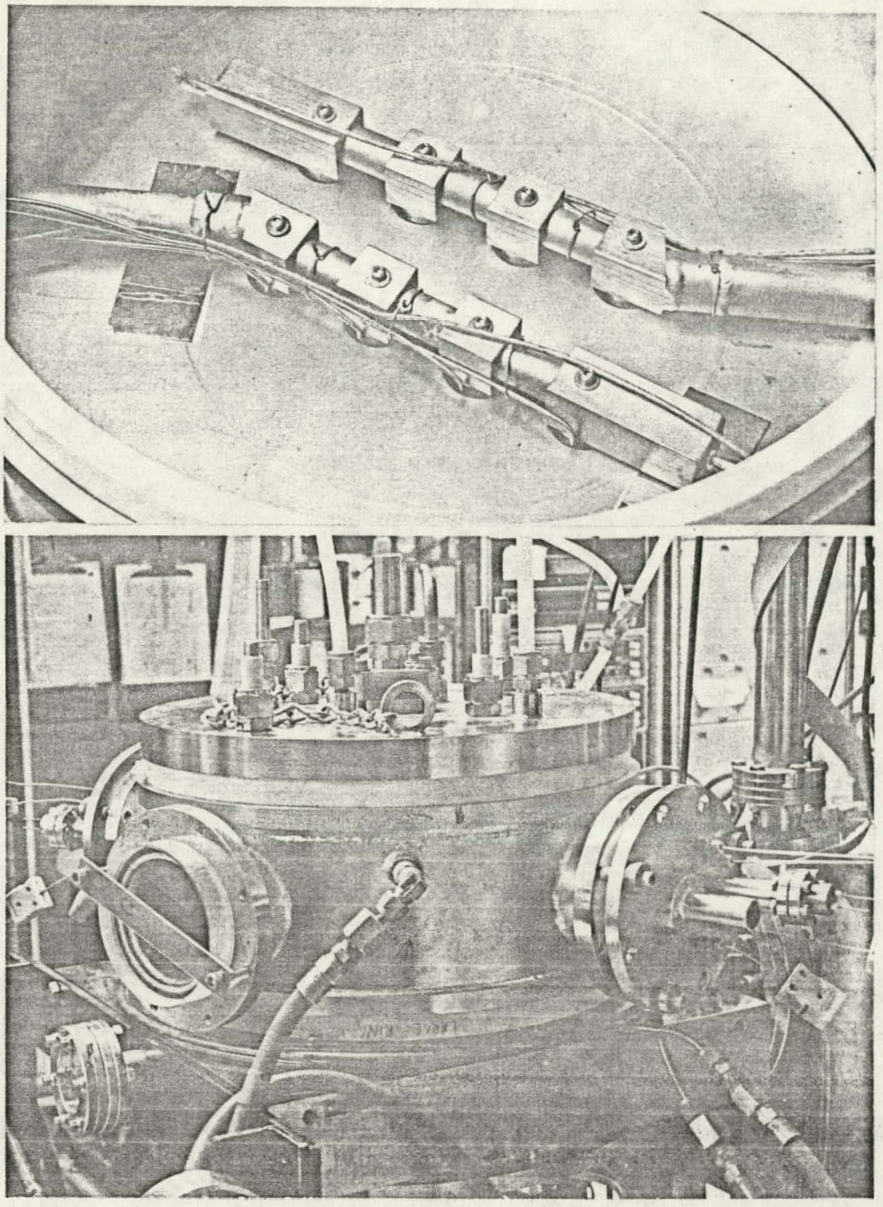

FIGURE 4

Apparatus for multiple specimen etch experiments. Top -- Back side of substrate support arms. Four specimens are mechanically attached to each arm with bolts. The temperature of each specimen is monitored with separate thermocouples while a temperature gradient is maintained with a heater placed at one end and forced-air cooling at the other. Etching is limited to the faces of the substrates by a plasma shield, shown here as a flat plate with the support arms resting on it and the circular substrates centered in holes thru it. Bottom -- Sputtering chamber with arms for etch experiments installed. Plasma is provided with a standard PNL lower base unit.

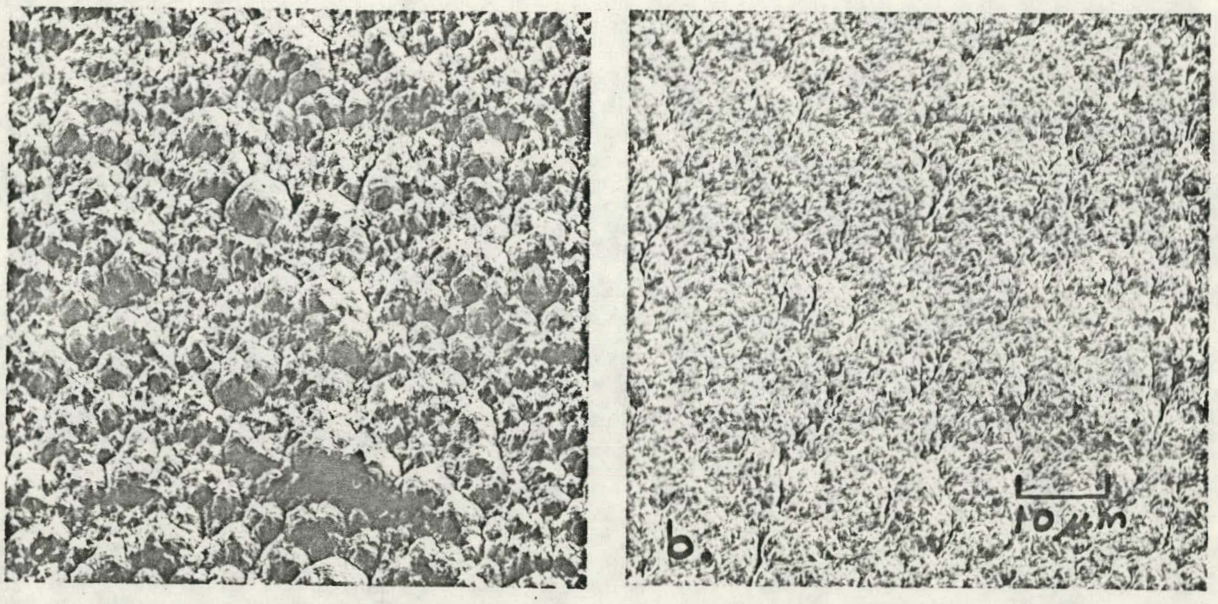

FIGURE 20

Surface features of stabilized zirconia sputter-deposited onto an unetched CoCrAlY bond coat. (a) Substrate surface features were similiar to Figure 19(d), ZrO_2 was rf biased during the deposition. (b) Substrate surface features were similiar to Figure 18, ZrO_2 was not rf biased during the deposition. 1200x. The thermal shock testing described in the text had no effect on the as-deposited surface features.

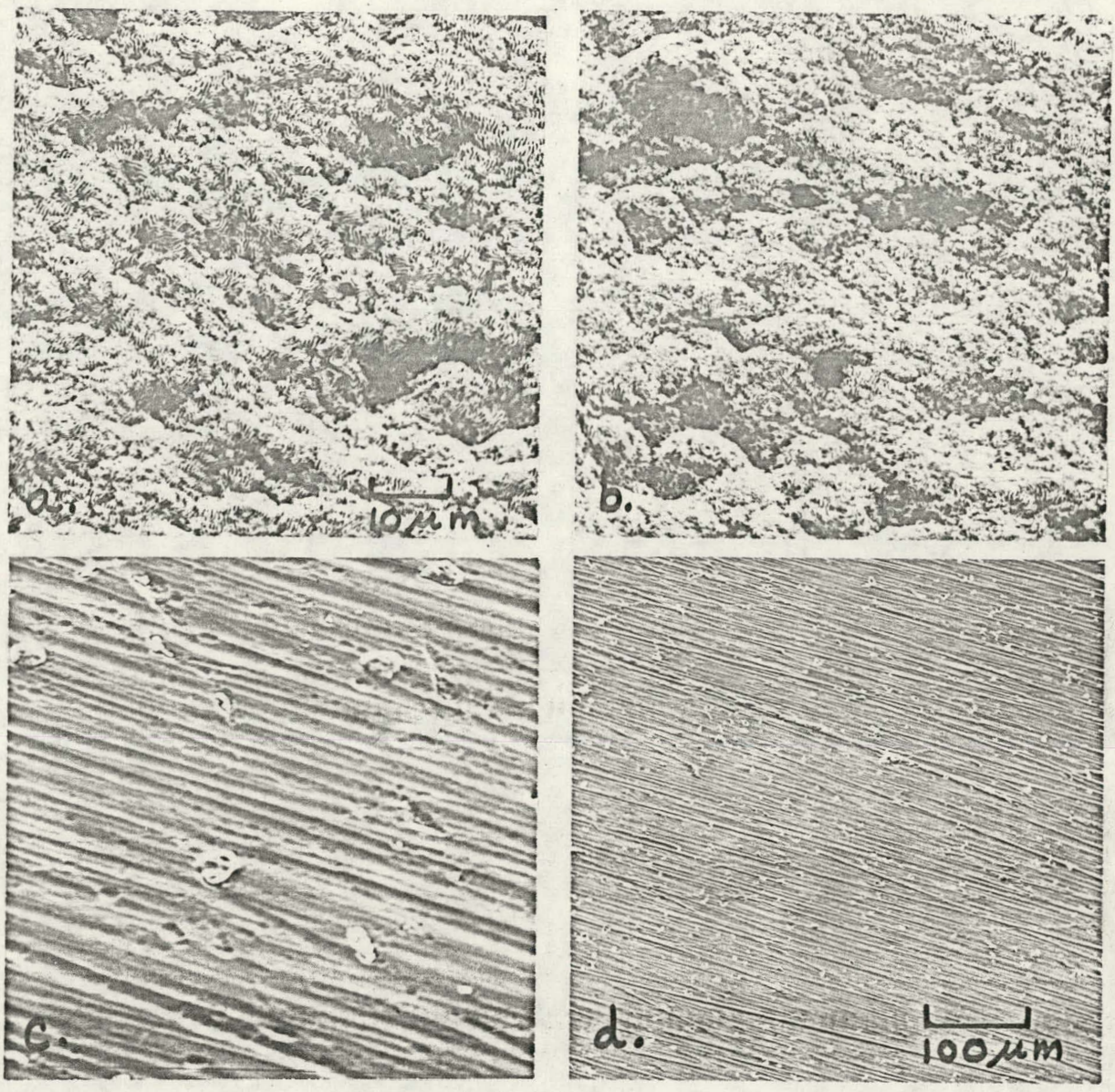

FIGURE 5
Surface features of IN718 formed by krypton-ion etching at 1000eV bias: (a) 490°C, 6.3 mamp/cm^2, 1200x; (b) 600°C, 6.3 mamp/cm^2, 1200x; (c) initial substrate surface, 1200x; (d) initial substrate surface, 150x.

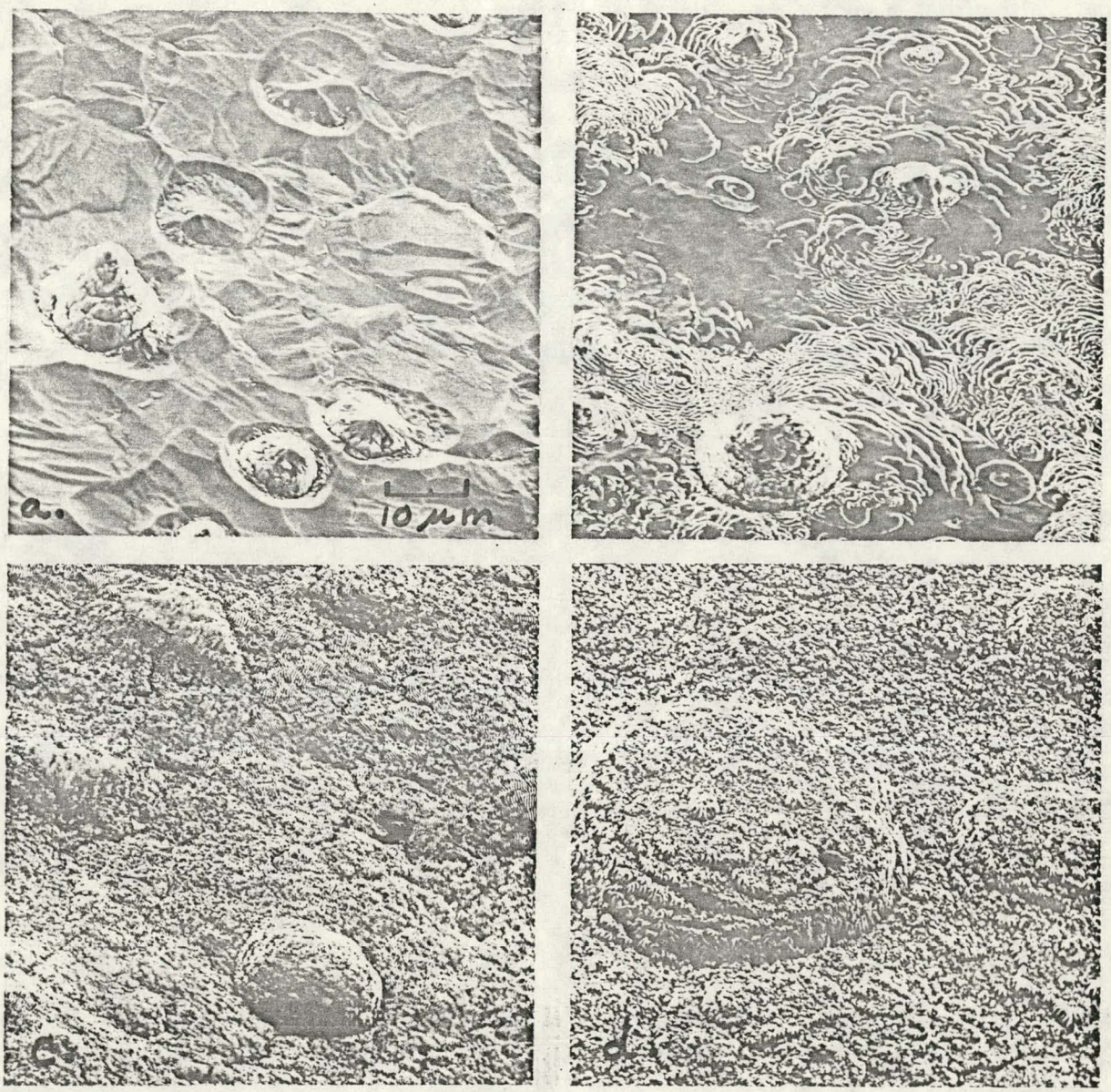

FIGURE 6
Surface features of IN718 formed by krypton-ion etching at 500eV bias: (a) 350°C, 5.4 mamp/cm^2; (b) 430°C, 8.9 mamp/cm^2; (c) 485°C, 8.9 mamp/cm^2; (d) 510°C, 8.9 mamp/cm^2. All 1200x.

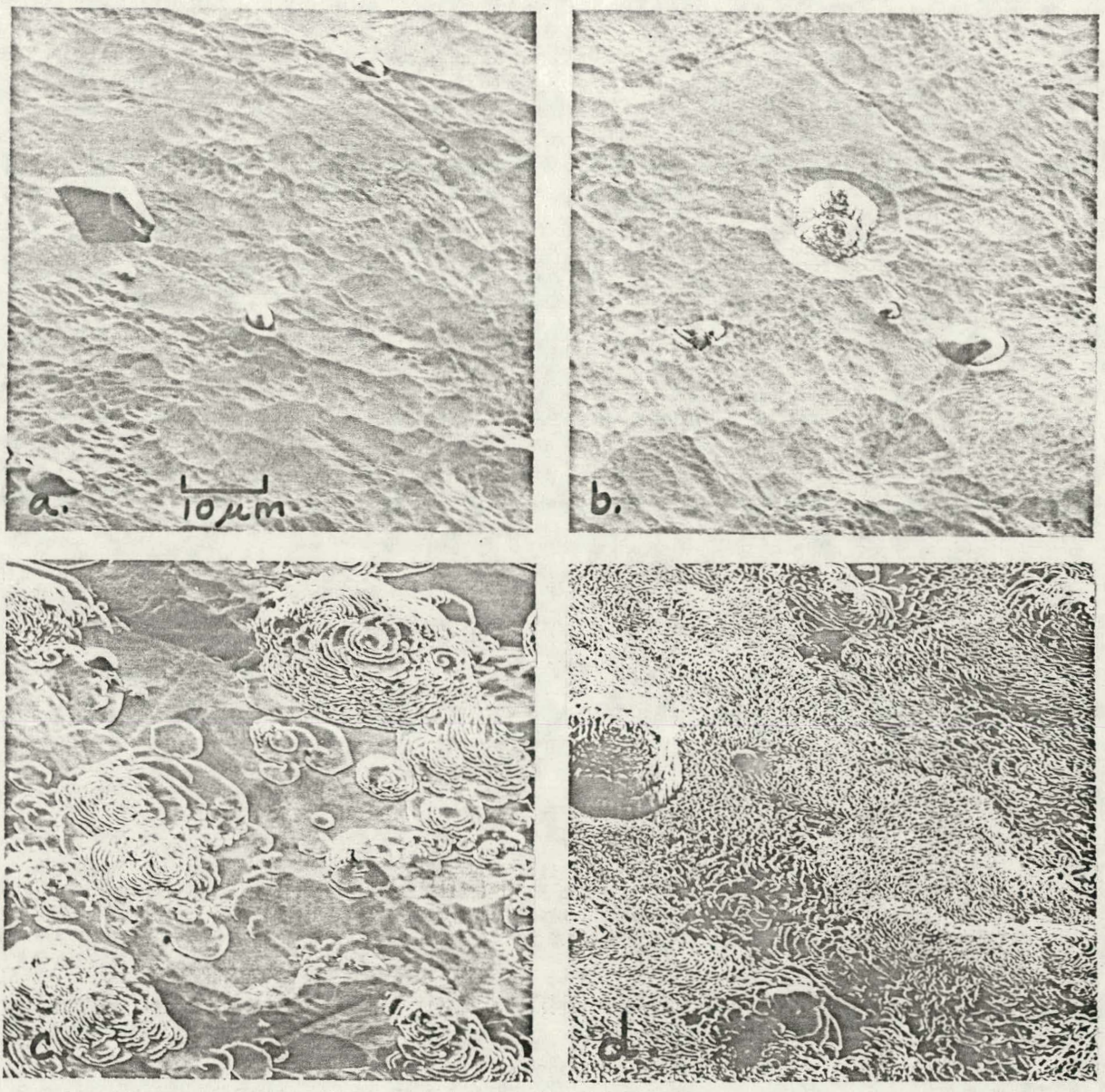

FIGURE 7
Surface features on IN718 formed by krypton-ion etching at 200eV bias: (a) 200°C, 7.2 mamp/cm^2; (b) 350°C, 5.1 mamp/cm^2; (c) 400°C, 4.7 mamp/cm^2; (d) 440°C, 7.9 mamp/cm^2. All 1200x.

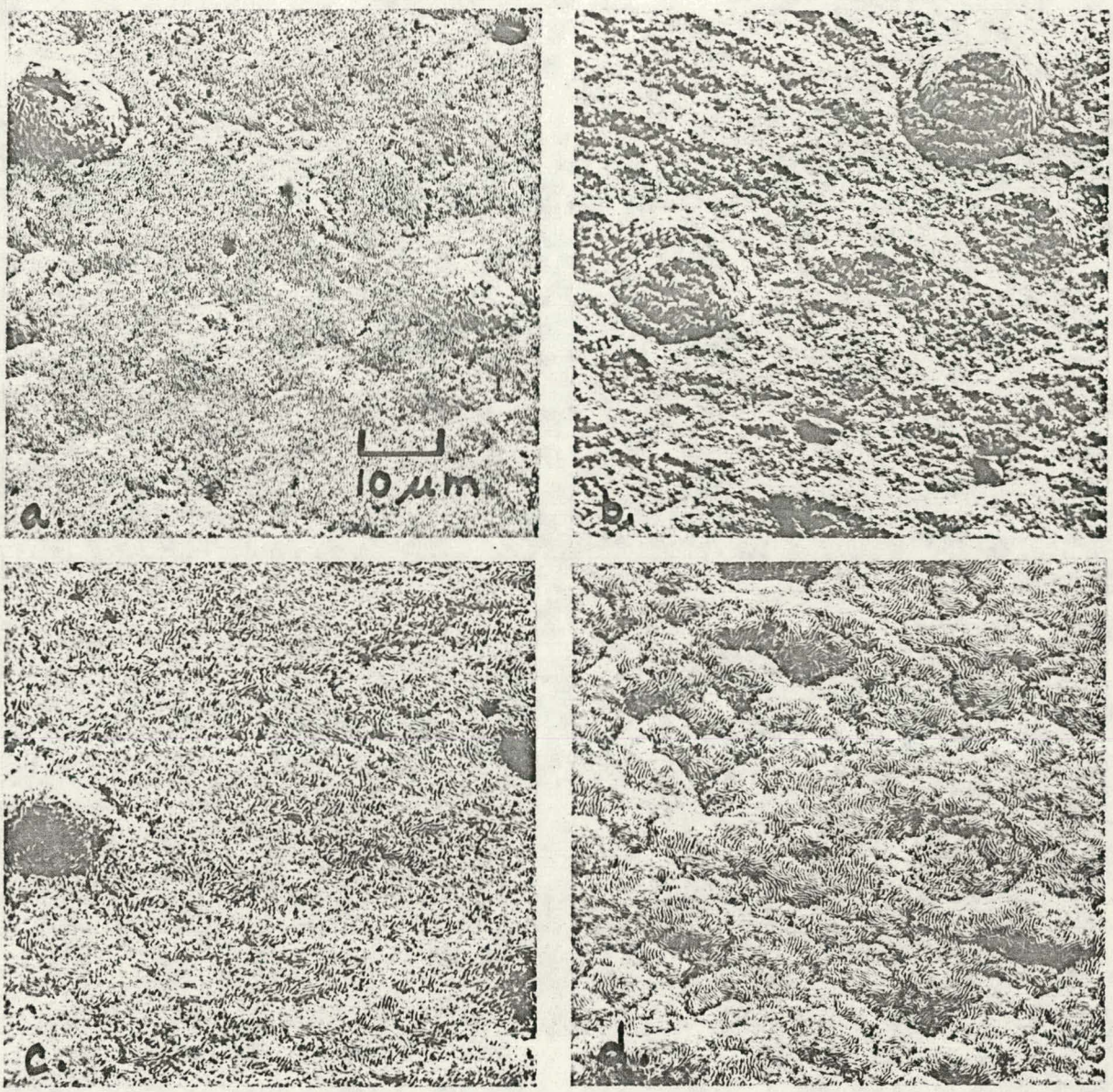

FIGURE 8
Surface features of IN718 seeded with $6x10^{14}$ to $2x10^{15}$ atoms/cm^2/sec of oblique incidence tantalum. (a) 400°C, 500eV Kr+, 7.6 mamp/cm^2; (b) 525°C, 500eV Kr+, 7.6 mamp/cm^2; (c) 525°C, 1000eV Kr+, 7.7 mamp/cm^2; (d) 585°C, 1000eV Kr+, 7.7 mamp/cm^2. All 1200x.

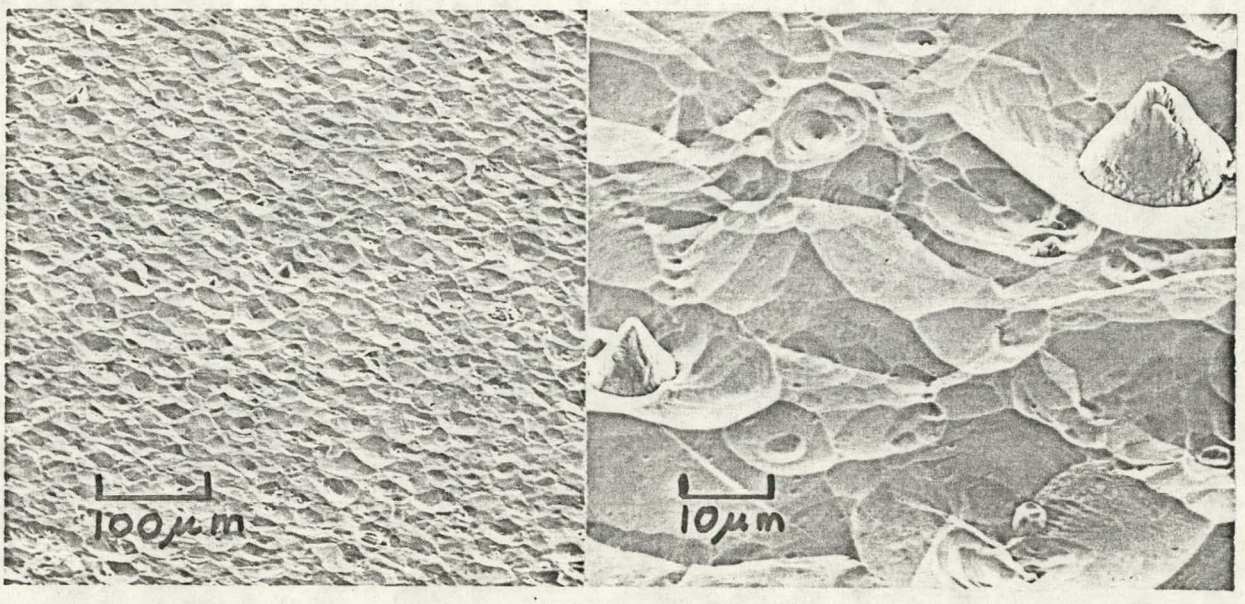

FIGURE 9
Cone growth on IN718 at 525°C with Mo and O_2 seeding. The Molydebum flux of about $2x10^{15}$ atoms/cm^2/sec arrived at about 20° angle of incidence, oxygen input was 2 cm^3/min (STP). Left 150x, right 1200x.

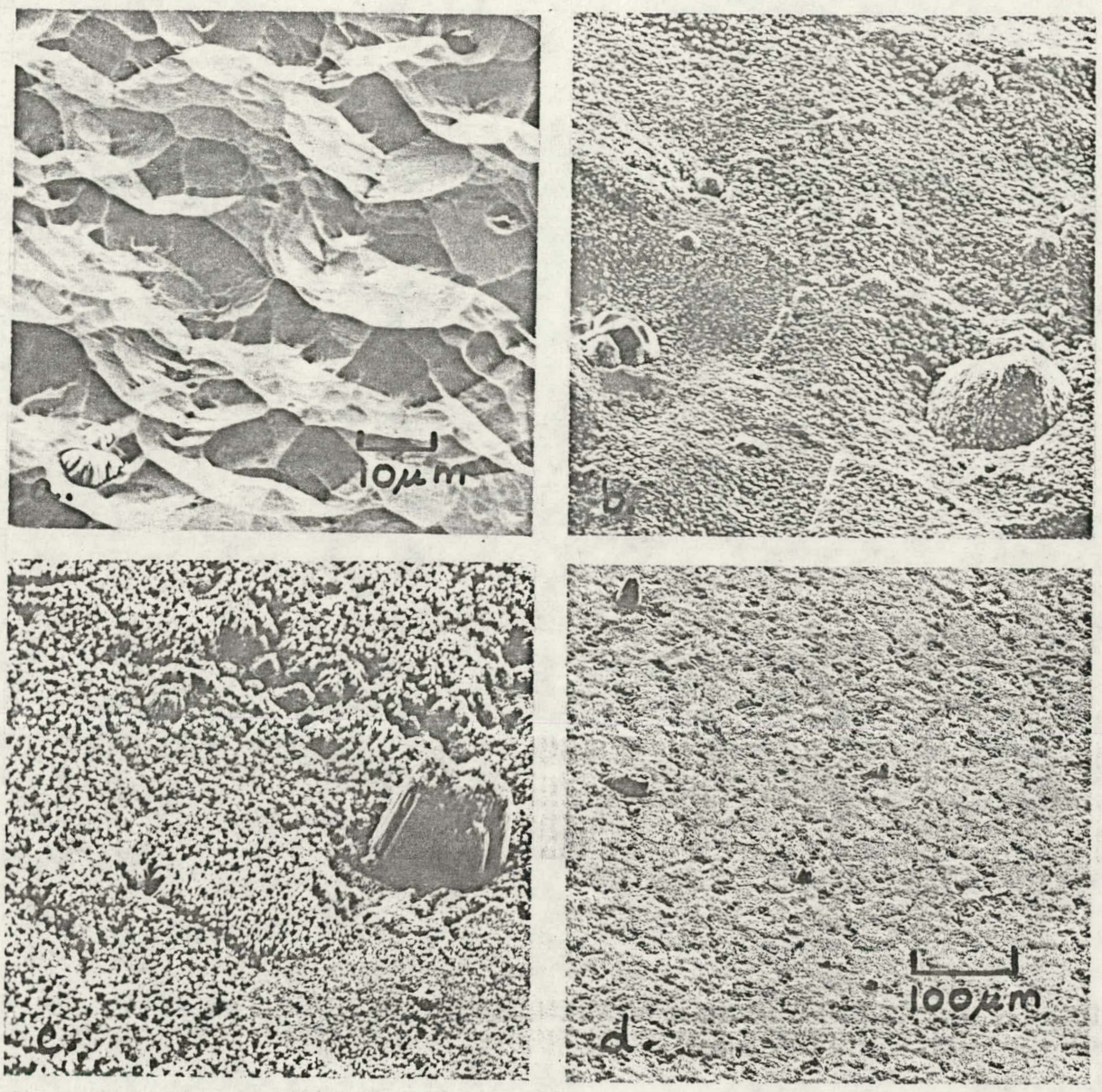

FIGURE 10

Surface features of IN718 seeded with oxygen. (a) 500eV, 470°C, 5.0 mamp/cm^2, 2 cm^3/min (STP) O_2; (b) 1000eV, 525°C, 5.4 mamp/cm^2, 1 cm^3/min (STP) O_2; (c,d) 1500eV, 485°C, 8.2 mamp/cm^2, 1 cm^3/min (STP) O_2; a,b,c = 1200x; d = 150x.

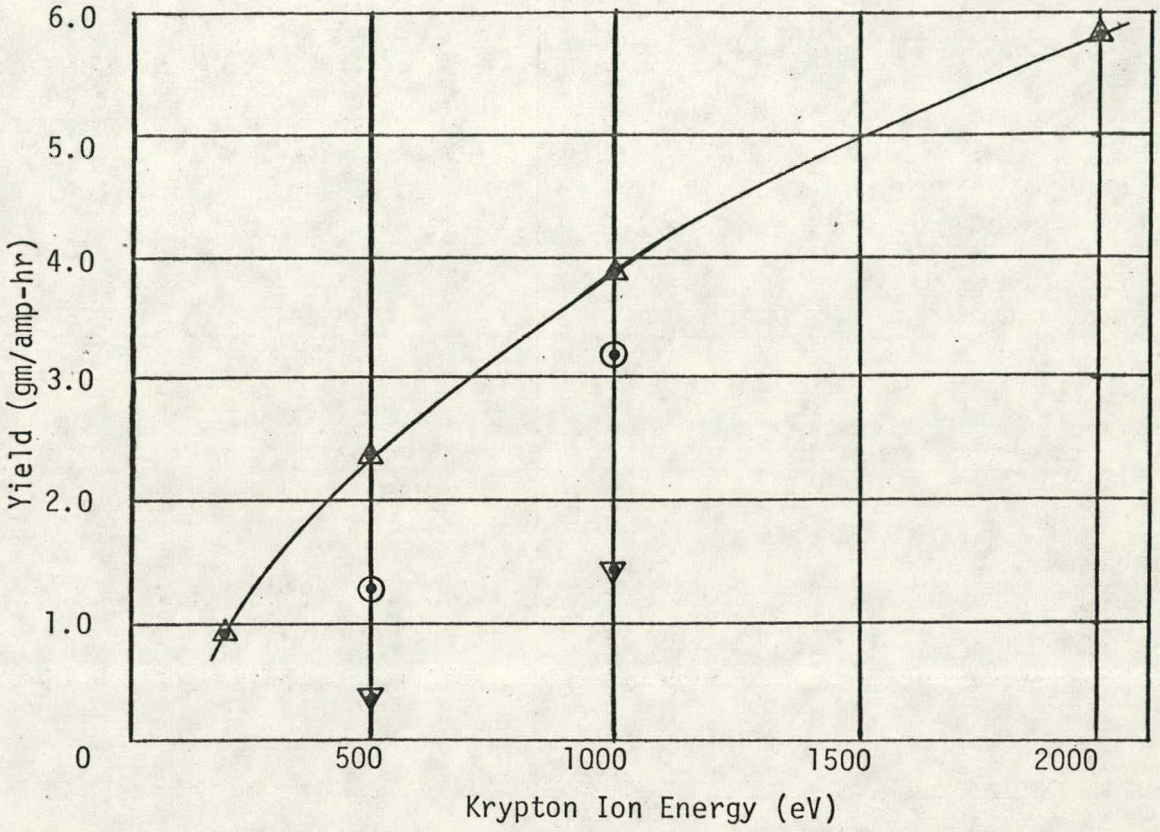

FIGURE 11

Sputtering yield of IN718 with krypton ions. The solid line is with water cooling. ⊙ is with 2 cm^3/min (STP) O_2 and temperatures above 400°C. ▽ is with 3 cm^3/min (STP) O_2 and temperatures above 360°C. Krypton flow is 0.7 cm^3/min (STP).

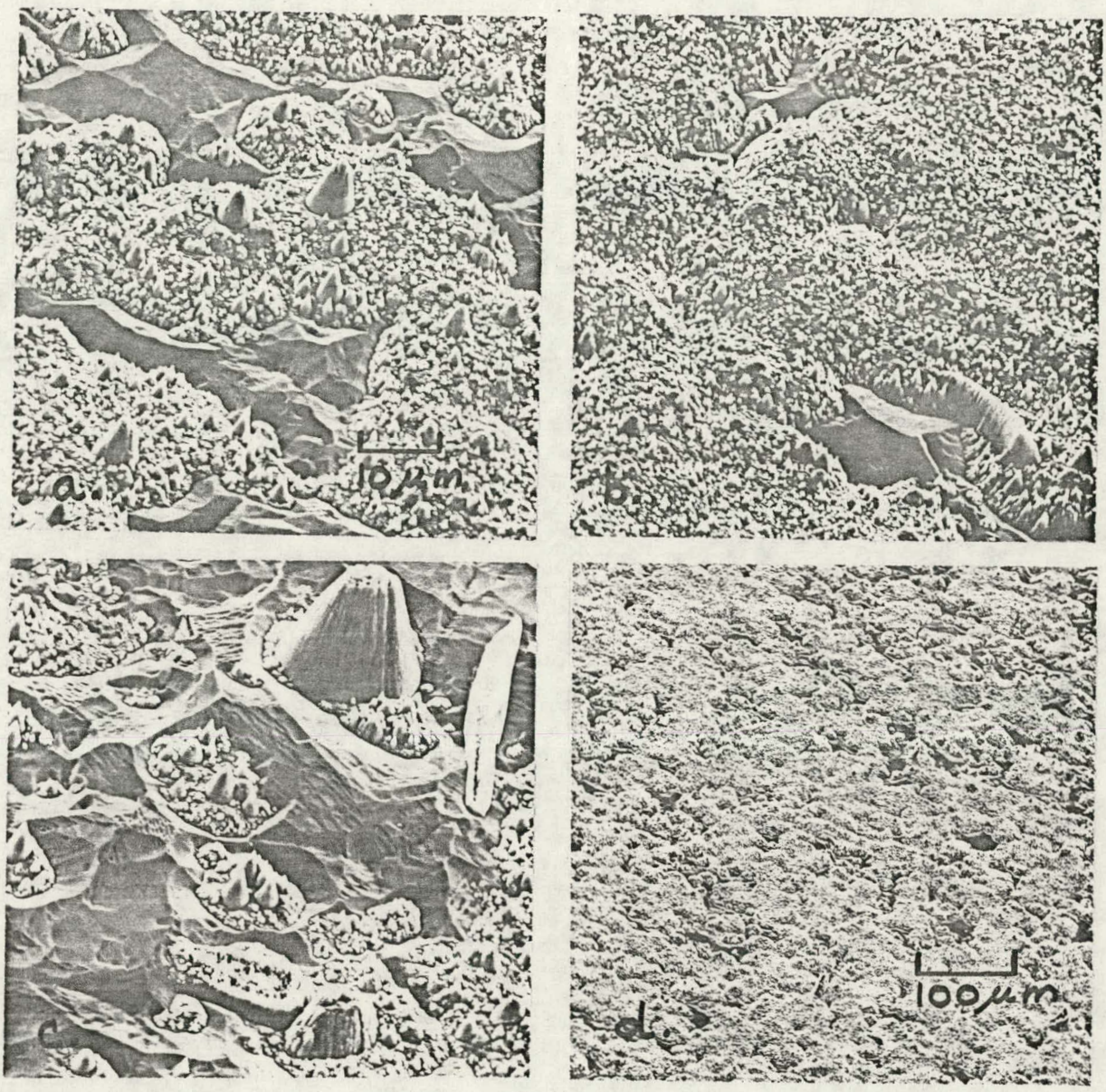

FIGURE 12
Surface features of IN718 seeded with oxygen and with suspected carbon surface contamination. Etched with 1000eV Kr+, 5.3 mamp/cm^2, 2 cm^3/min (STP) O_2. (a) 530°C; (b,d) 590°C; (c) 610°C; a,b,c are 1200x; d is 150x.

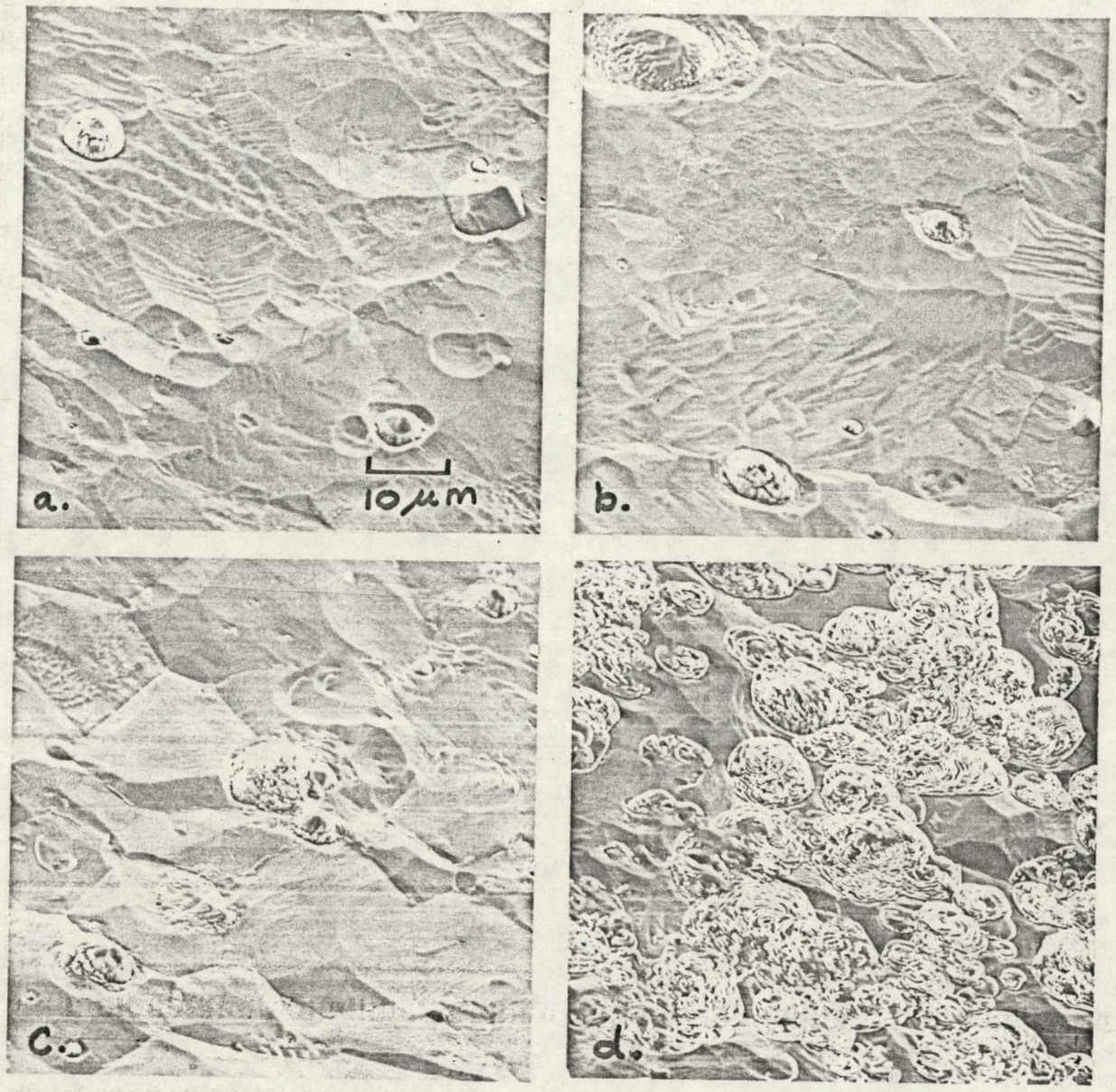

FIGURE 13
Surface features of IN718 seeded with Starrett oil in toluene. Etched with 500eV Kr+, 5.4 mamp/cm^2. (a) 360°C; (b) 430°C; (c) 460°C; (d) 515°C; 1200x.

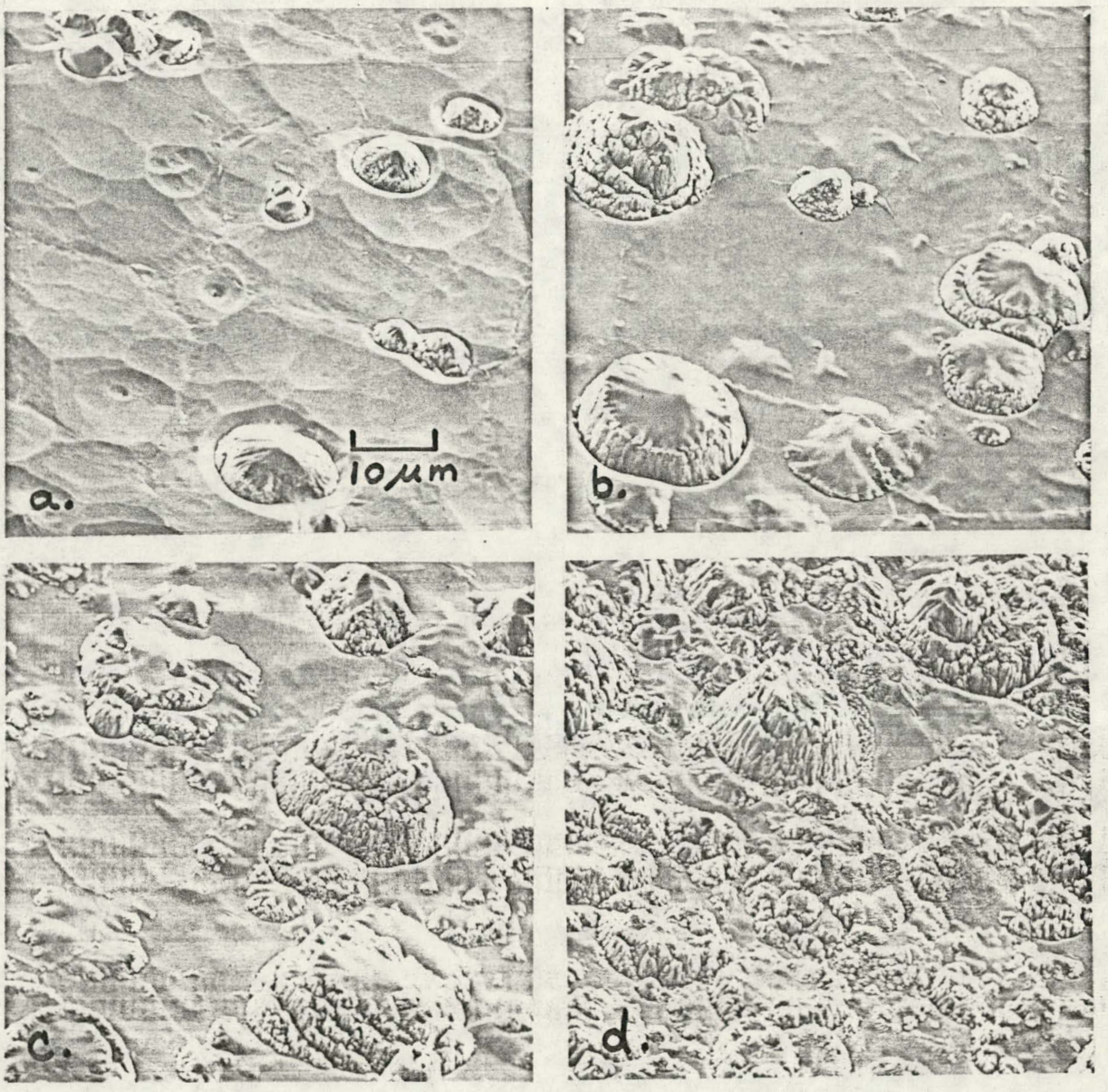

FIGURE 14
Surface features of IN718 seeded with Starrett oil in toluene. Etched with 1000eV Kr+, 6.4 mamp/cm^2. (a) 360°C; (b) 430°C; (c) 460°C; (d) 515°C; 1200x.

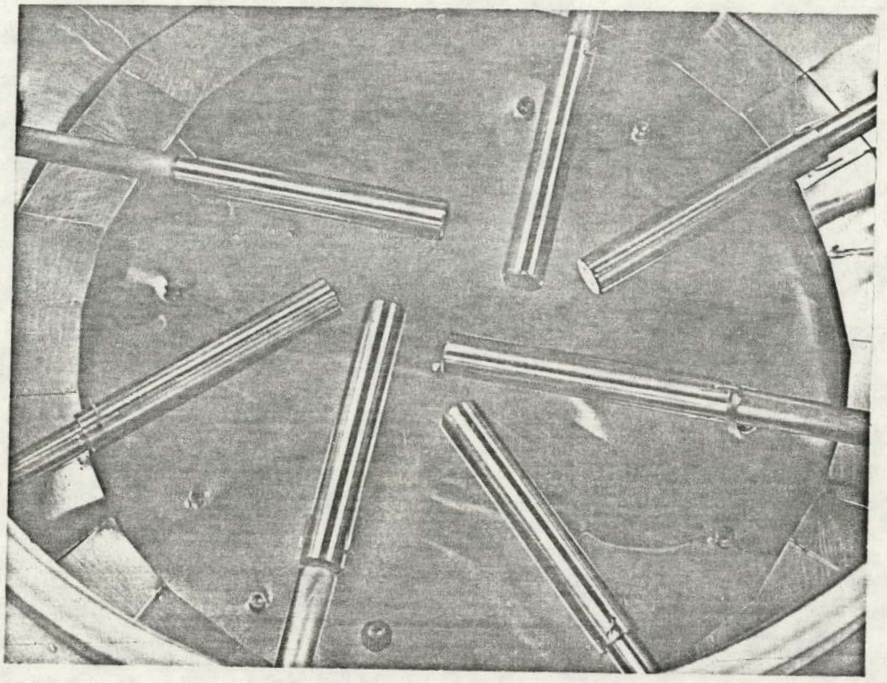

FIGURE 15
Substrates installed on rotating holders in sputter-deposition apparatus.

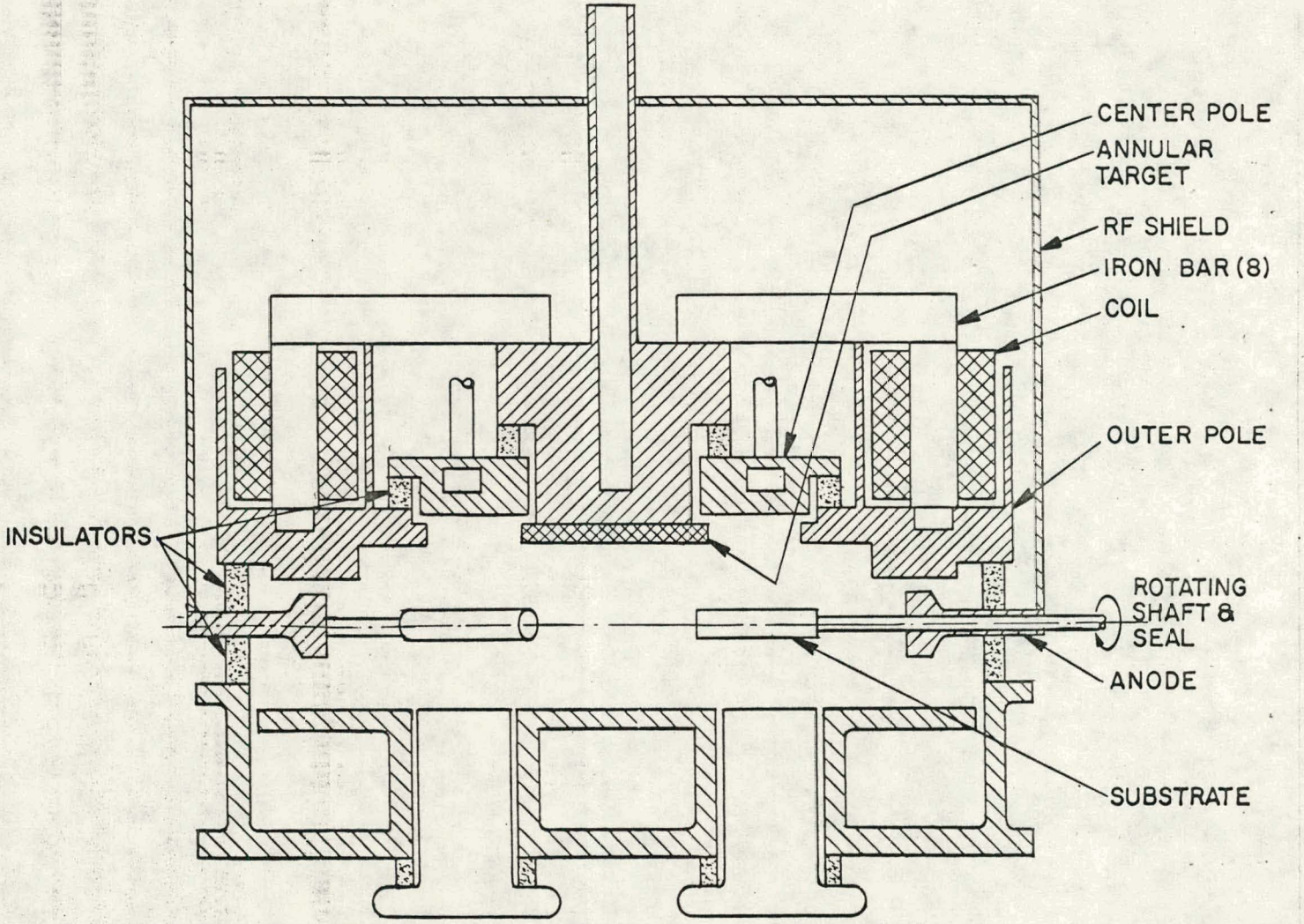

FIGURE 16

Modified planar magnetron sputtering apparatus for high-rate compound or reactive sputtering. Target ion current densities in excess of 80 mamp/cm^2 with a D C floating potential up to 2400 volts can be achieved.

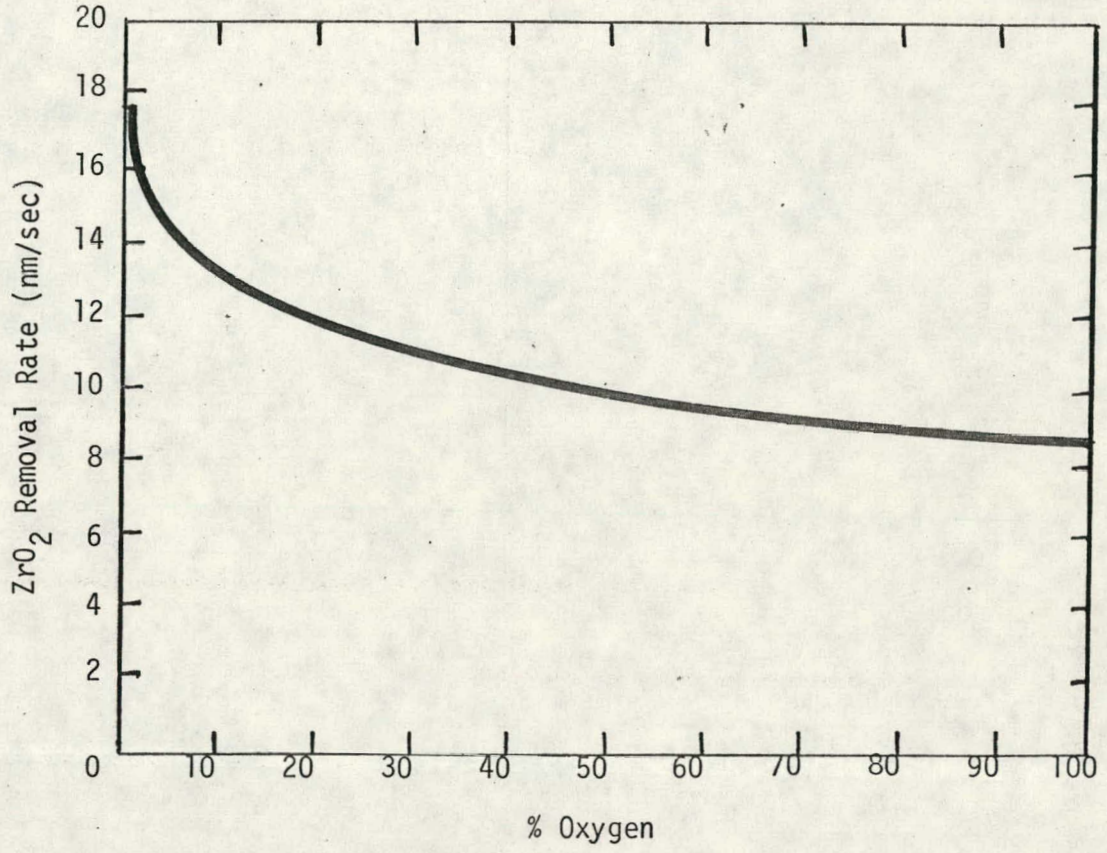

FIGURE 17

Achievable target removal rate for zirconia with krypton/oxygen mixtures in the modified planar magnetron. Both the sputtering yield and the target current density depend on the oxygen partial pressure in the modified planar magnetron sputtering apparatus.

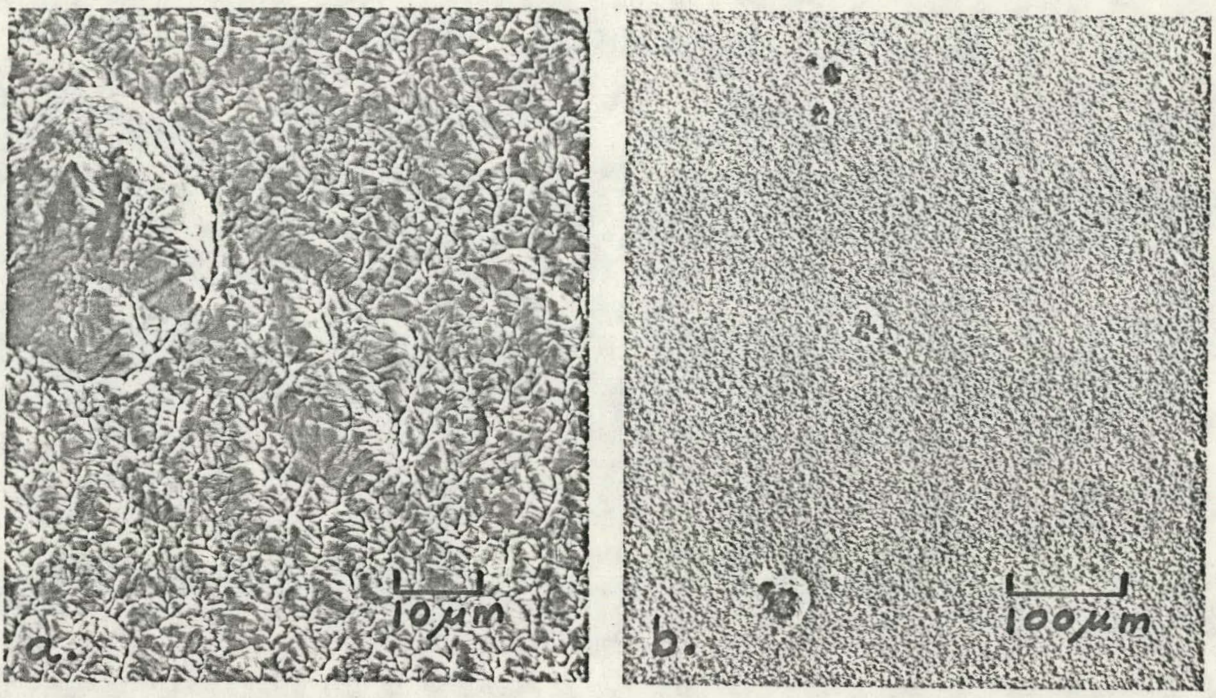

FIGURE 18
Topography of CoCrAlY deposited onto rotating tubular stainless steel substrates. (a) 1200x; (b) 150x.

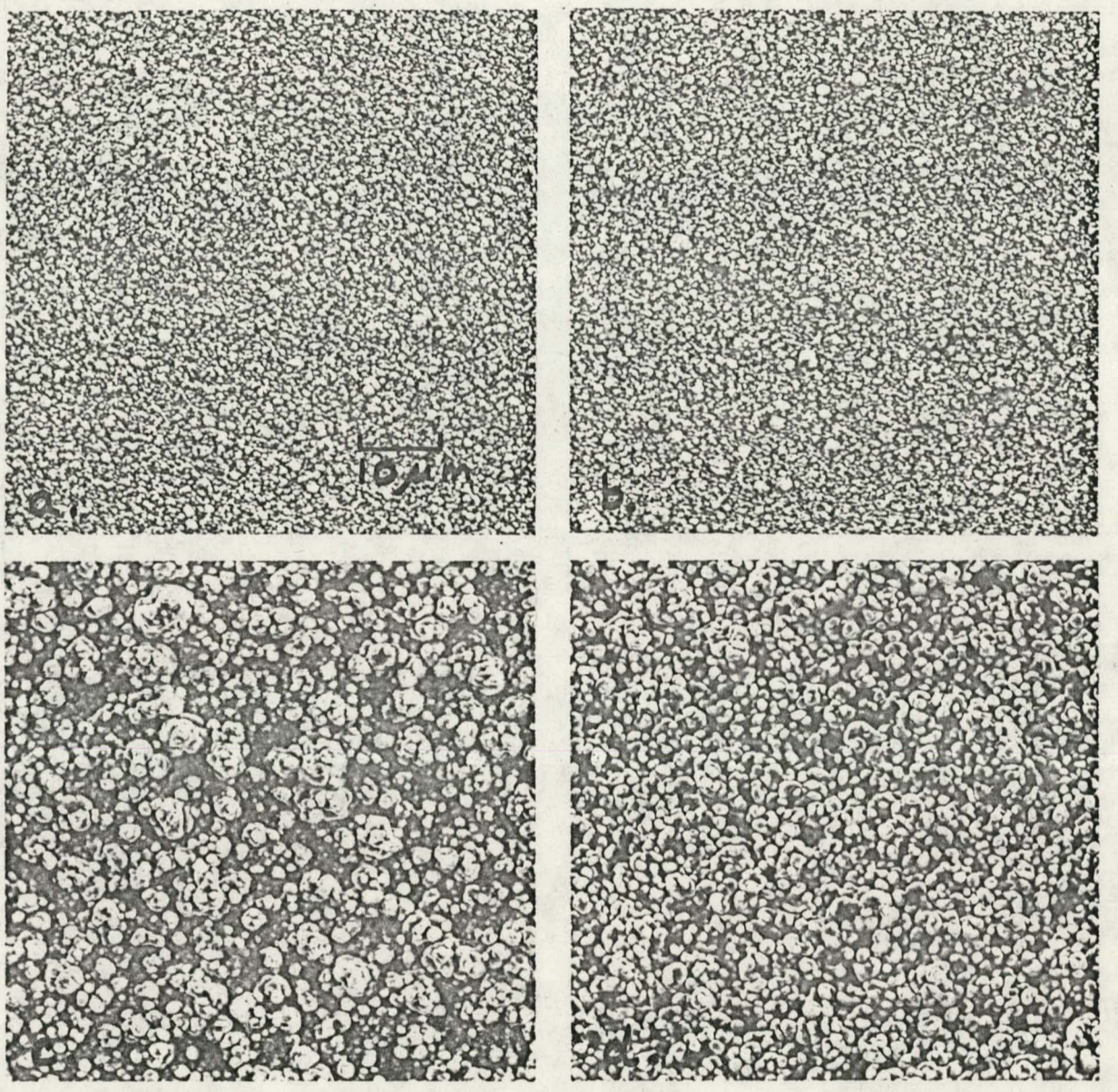

FIGURE 19
Surface features of CoCrAlY without foreign atom seeding. (a) 100eV Kr+, 600°C, 6.6 mamp/cm^2; (b) 200eV Kr+, 620°C, 4.8 mamp/cm^2; (c) 300eV Kr+, 830°C, 7.4 mamp/cm^2; (d) 500eV Kr+, 765°C, 5.4 mamp/cm^2; 1200x.